Spin−Orbit Coupling Effects on the Metal−Hydrogen Bond Homolysis of $M(H)(CO)_3$(H-DAB) (M = Mn, Re; H-DAB = 1,4-Diaza-1,3-butadiene)

Chantal Daniel* and Dominique Guillaumont

Laboratoire de Chimie Quantique, UMR 7551 du CNRS et de l'Université Louis Pasteur, Institut Le Bel, 4 Rue Blaise Pascal, 67 000 Strasbourg, France

Carl Ribbing

Department of Chemistry, Katholieke Universiteit Leuven, Leuven, Belgium

Boris Minaev

Cherkassy Engineering and Technological Institute, Cherkassy, Ukraine

Received: November 12, 1998

The spin−orbit coupling (SOC) induced mixing between the low-lying singlet and triplet electronic excited states of $M(H)(CO)_3$(H-DAB) (H-DAB = 1,4-diaza-1,3-butadiene) (M = Mn, Re) is investigated through SOC-CI calculations, using a one-electron effective spin−orbit operator at the metal center. On the basis of the spin−orbit interactions calculated between the low-lying singlet and triplet $nd \rightarrow \pi^*_{DAB}$ (Metal-to-Ligand Charge Transfer) and $\sigma_{M-R} \rightarrow \pi^*_{DAB}$ (Sigma-Bond-to-Ligand Charge Transfer) excited states, it is shown how the spin−orbit effect may control the metal−hydrogen bond breaking of this class of complexes. In the manganese complex, the spin−orbit interactions between the low-lying singlet and triplet states range between 0 and 100 cm^{-1}, whereas in the rhenium complex they are calculated between 100 and 560 cm^{-1}. The spin−orbit splitting of the lowest triplet excited states is negligible in the manganese complex with values of a few tens of wavenumbers, whereas it becomes significant (between 80 and 1200 cm^{-1}) in the rhenium complex. The spin−orbit interactions between the ^{1}MLCT state, populated after visible irradiation, and the ^{3}SBLCT state, dissociative for the metal hydrogen bond homolysis, are estimated at 75 and 314 cm^{-1} in the manganese and rhenium complexes, respectively. In order to evaluate the consequence of the spin−orbit interaction increase on the probability of dissociation of the M−H bond through ^{1}MLCT → ^{3}SBLCT intersystem crossing, preliminary wave packet propagations have been performed on idealized spin−orbit coupled potentials in the diabatic representation with coupling terms of 500 and 80 cm^{-1}. In both cases the metal−hydrogen bond breaking probability never exceeds 1% in 1 ps.

1. Introduction

On the basis of detailed spectroscopic, photophysical, and photochemical investigations[1−8] of a series of complexes $M(L)(CO)_3$(α-diimine) (M = Mn, Re), in which L represents a metal fragment or an alkyl group bound to the metal by a high-lying σ orbital, it was concluded that mainly $d\pi(M) \rightarrow \pi^*$(α-diimine) (MLCT) transitions contribute to the absorption spectra and that emission and homolysis reactions take place from a close low-lying $\sigma_{M-L} \rightarrow \pi^*$(α-diimine) (^{3}SBLCT) excited state. A tentative rationalization of the experimental data based on accurate CASSCF/MR-CCI calculations[9−11] of the low-lying excited states of $M(R)(CO)_3$(H-DAB) (M = Mn, R = H, methyl, ethyl; M = Re, R = H), completed by a careful analysis of the potential energy surfaces for $Mn(H)(CO)_3$(H-DAB),[12,13] has been proposed. The interaction between the quasi-bound MLCT excited states and the SBLCT excited state dissociative for the metal−hydrogen bond breaking is the key of the photochemical behavior observed in this class of molecules (Figure 1). Indeed, the presence of energy barriers due to avoided crossings between the two ^{3}MLCT states and the ^{3}SBLCT state at the early stage of the reaction pathway corresponding to the Mn−H homolysis prevents the occurrence of this reaction in the hydride complex. This qualitative interpretation has been corroborated by a recent wave packets simulation of the dynamics of the MLCT excited states of $Mn(H)(CO)_3$(H-DAB) performed on the two-dimensional potential energy surfaces calculated as a function of the Mn−H and $Mn-Co_{axial}$ bonds elongations.[11] The axial CO loss appears to be the major process after 300 fs of simulation, the Mn−H bond homolysis being inhibited by the bound character of the MLCT states along this dissociative channel. Unfortunately, these results cannot be compared directly to the experimental data for two reasons: (i) the synthesis of the hydride complex has not been successful; (ii) femtosecond experiments are emerging for these molecules. However, this mechanism explains the low photoreactivity of the methyl analogue $Mn(CH_3)(CO)_3$(H-DAB).[8] The quantum yield and the time scale of the homolysis in this class of molecules will depend on the factors (wavelength of irradiation, nature of the radical species to be produced, metal center, and π-acceptor ligand) governing the energy barriers height.

An illustration of this unconventional photochemical/photophysical behavior has been recently reported for a number of manganese and rhenium complexes. For instance, whereas the homolysis of $M(R)(CO)_3$(α-diimine) (M = Re with R = ethyl, benzyl or M = Mn with R = benzyl; α-diimine = R′-DAB, R′

10.1021/jp984418j CCC: $18.00
Published on Web 07/03/1999

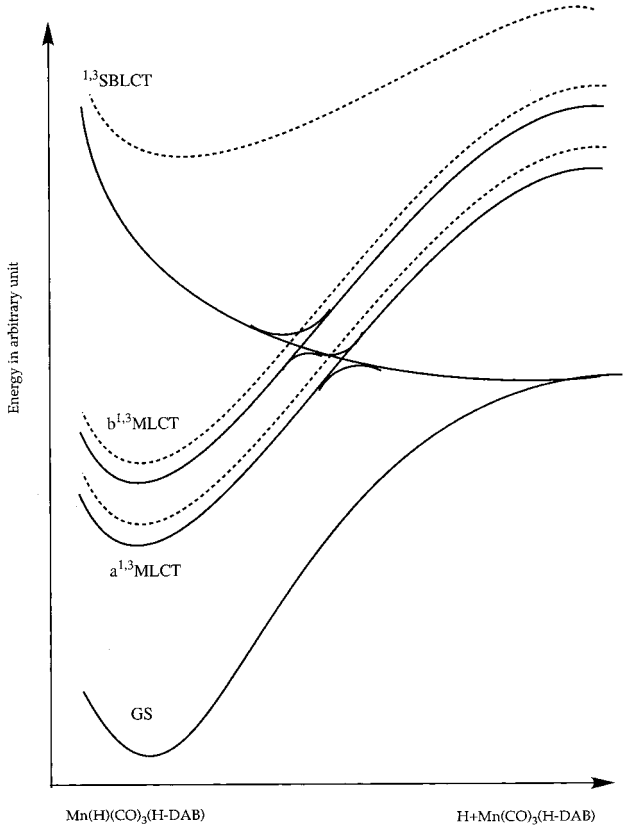

Figure 1. Idealized potential energy curves (PEC) of the ^{1,3}SBLCT and low-lying ^{1,3}MLCT states along the coordinate corresponding to the Mn−H homolysis in Mn(H)(CO)$_3$(H-DAB).

= iPropyl, pTol) is characterized by a quantum yield close to 1, the methyl analogues do not show significant homolysis upon visible excitation ($\phi \approx 10^{-2}$ for M = Re,[7] $\phi = 0$ for M = Mn[8]). When the α-diimine ligand is replaced by a substituted bipyridine in Re(R)(CO)$_3$(bpy′), the branching ratios between the homolysis and the emission to the electronic ground state are 0.40/0.60 and 1.0/0.0 for the methyl and the ethyl complexes, respectively.[14] More generally, the rhenium complexes are more photoreactive with respect to the metal−hydrogen bond homolysis than the manganese analogues.[15]

The theoretical study of the influence of the ligand R on the photoreactivity of Mn(R)(CO)$_3$(H-DAB) has been recently discussed in detail.[9] Another important influencing factor is the nature of the metal center. A detailed comparative study of the low-lying excited states of Mn(H)(CO)$_3$(H-DAB) and Re(H)-(CO)$_3$(H-DAB) indicates that the substitution of the first-row transition metal atom by a rhenium atom has two significant consequences:[10,11] (i) a lowering of the excited states, and (ii) an important mixing between the so-called MLCT and SBLCT states.

The aim of the present contribution is to focus on the importance of the spin−orbit coupling effects on the metal−hydrogen bond breaking in these two model complexes (tentatively prepared) through spin−orbit-coupling configuration Interaction (SOC-CI) calculations based on CASSCF reference wave functions. This investigation is performed in the context of an extensive theoretical study based on quantum chemistry and dynamics and carried out for several M(R)(CO)$_3$(α-diimine) systems with R = H, methyl, or ethyl, and M = Mn, Re.[9−13] The rationalization of the influence of the metal center on the photophysical/photochemical properties of the M(R)(CO)$_3$(α-diimine) complexes is the ultimate goal of this study.

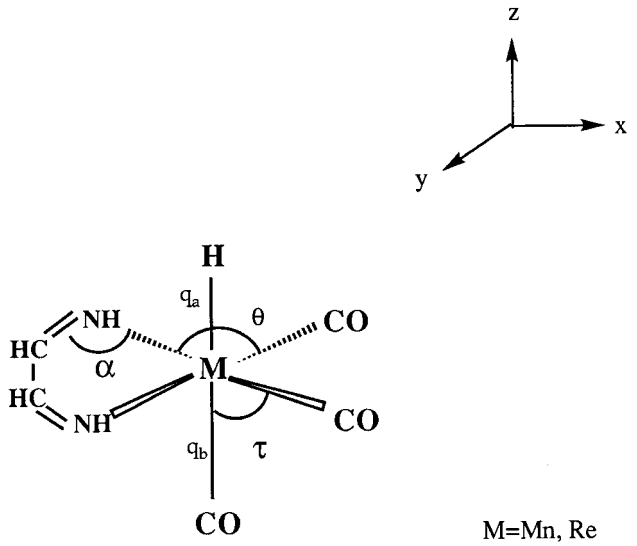

Figure 2. Idealized geometry of M(H)(CO)$_3$(H-DAB) (M = Mn, Re).

2. Computational Method

The calculations have been performed under the C_s symmetry constraint for the ^{1}A′ electronic ground state corresponding to the $(\sigma_{Mn-H})^2(nd_{x^2-y^2})^2(nd_{yz})^2(nd_{xz})^2$ electronic configuration (n = 3 for the manganese complex, n = 5 for the rhenium) and for the low-lying ^{1,3}A′ excited states corresponding to the $nd_{xz} \rightarrow \pi^*_{DAB}$, $nd_{x^2-y^2} \rightarrow \pi^*_{DAB}$ and $\sigma_{Mn-R} \rightarrow \pi^*_{DAB}$ excitations in M(H)(CO)$_3$(H-DAB) with the conformations depicted in Figure 2. Idealized geometries were deduced from the ground state structures of MnCl(CO)$_3$(DAB),[16] HMn(CO)$_5$,[17] and Re(R)-(CO)$_3$(iPr-DAB)[18] with the following bond lengths and bond angles:

For Mn(H)(CO)$_3$(DAB): Mn−H = 1.576 Å, Mn−CO$_{ax}$ = 1.820 Å; Mn−CO$_{eq}$ = 1.807 Å; DAB: Mn−N = 2.032 Å, N−C = 1.280 Å; C−C = 1.508 Å, N−H = 1.010 Å; C−H = 1.080 Å, the angles τ, θ, and α being kept constant to 90°, 96° and 117, 5°, respectively.

For Re(H)(CO)$_3$(DAB): Re−H = 1.799 Å; Re−CO = 2.000 Å; DAB: Re−N = 2.177 Å, the angles τ, θ, and α being kept constant to 96.3°, 98°, and 113, 1°, respectively.

In a recent work,[19] we have shown that the geometrical structure of Mn(H)(CO)$_3$(DAB) is not significantly affected on going from the electronic ground state to the lowest triplet excited states. On the basis of these results and of the experimental findings (a very small shift of the absorption/emission spectra in these molecules[15]), a systematic geometry optimization of the triplet excited states is not justified.

The following Gaussian basis sets were used for Mn(R)(CO)$_3$-(DAB) in an all-electron calculation scheme: for the manganese atom a (15,11,6) set contracted to [9,6,3],[20] for the first-row atoms a (10,6) set contracted to [4,2],[23] for hydrogen atom either a (6,1) set contracted to [3,1] [24] (for the atom directly linked to the metal center) or a (4) set contracted to [2] [23] for the other hydrogen atoms. For the rhenium complex the metal atom alone is described in the relativistic ab initio model potential method (CG-AIMP).[25] The following Gaussian basis sets based on atomic natural orbitals[26] were used: for the rhenium atom (Z = 13.0) a (13, 10, 9, 5) set contracted to [3,3,4,2],[25] for the carbon (all-electrons), nitrogen (all-electrons) and oxygen (all-electrons) atoms a (10,4,3) set contracted to [3,2], for the hydrogen atoms a (7,3) set contracted to [2].

TABLE 1: CASSCF/SOC-CI and CASSCF/MR-CCI Excitation Energies (in cm^{-1}) to the Low-Lying $^{1,3}A'$ Excited States of $Mn(H)(CO)_3$(H-DAB) and Spin−Orbit (SO) Splitting (in cm^{-1})

transition	CASSCF/-SOC-CI	SO splitting	CASSCF[a]	CASSCF/-MR-CCI[a]
$a^1A' \rightarrow a^3A'$				
a^3MLCT	14 075	30−60	12 900	15 090
$a^1A' \rightarrow b^3A'$				
b^3MLCT	17 520	10	16 390	19 200
$a^1A' \rightarrow b^1A'$				
a^1MLCT	17 530	0	17 500	21 060
$a^1A' \rightarrow c^1A'$				
b^1MLCT	21 000	0	21 000	26 000
$a^1A' \rightarrow c^3A'$				
^{3}SBLCT	30 520	3	29 120	34 390
$a^1A' \rightarrow d^1A'$				
^{1}SBLCT	32 770	0	32 750	37 950

[a] Reference 10.

CASSCF calculations [27] were carried out to obtain wave functions which are used as references in the SOC-CI calculations based on a restricted full CI scheme.[28] CASSCF calculations averaged over three to five low-lying states of the ground state symmetry A′ for a given spin have been performed in order to generate a set of molecular orbitals used in the subsequent SOC-CI. Since our interest centers mostly on the lowest excited states corresponding to nd $\rightarrow \pi^*_{DAB}$ and $\sigma_{M-R} \rightarrow \pi^*_{DAB}$ excitations, eight electrons are correlated (the nd electrons and the two electrons involved in the M−R bond) in 10 orbitals corresponding to the nd and nd′ orbitals which correlate them, the σ_{M-R} and σ^*_{M-R} orbitals (σ_{M-R} and σ^*_{M-R} denote the molecular orbitals that are bonding and antibonding with respect to the M−R bond, respectively) and the lowest π^*_{DAB} localized on the DAB group. The same active space has been defined in the SOC-CI calculation where eight electrons are correlated in a full-CI scheme for the manganese complex. The effective charges $Z^{K,i}_{eff}$ used in the one-electron effective spin−orbit operator (eq 1) where $r_{K,i}$ denotes the electron−nucleus distance, K the metallic center, l the valence shell azimuthal quantum number, and α the fine structure constant)

$$\hat{H}^{eff}_{so} = \sum_i \hat{A}^{(i)}\hat{S}^{(i)} \qquad (1)$$

of 15.0 and 60.0 for the manganese and the rhenium atoms, respectively, have been deduced from the experimental atomic splitting in the L−S coupling scheme.[29] The SOC-CI excitation energies obtained according to this limited computational strategy are compared to more accurate MR-CCI excitation energies reported elsewhere for the same molecules.[10] The integrals and wave functions calculations were performed either with the system of programs MOLCAS 3.0[30] or with ASTERIX.[31]

3. Results and Discussion

Spin−Orbit Effects in $Mn(H)(CO)_3$(H-DAB) . The CASSCF/SOC-CI excitation energies to the low-lying triplet and singlet excited states of $Mn(H)(CO)_3$(H-DAB) are reported in Table 1 together with the values obtained through the more accurate CASSCF/MR-CCI method.[10]

The SOC-CI excitation energies reproduce the CASSCF values within a few hundred wavenumbers depending on the nature of the optimized CASSCF reference wave function ($^1A'$ or $^3A'$). The large differences between the SOC-CI and the MR-CCI values are purely due to important dynamical correlation effects which are well described in the multireference approach. The neglect of these correlation effects in the restricted full-CI approach (SOC-CI) leads to errors on the excitation energies which may exceed 15%. This is especially true for the singlet excited states which need a large number of references to be described properly due to important mixing of configurations and to their interaction with the electronic ground state. However, the relative order of the transition energies and the nature of the excited states are not dramatically affected on going from the SOC-CI to the more refined treatment. Indeed, the low-lying singlet and triplet excited states are nearly pure and correspond to $3d_{xz} \rightarrow \pi^*_{DAB}$ and $3d_{x^2-y^2} \rightarrow \pi^*_{DAB}$ excitations. The singlet components contribute to the visible absorption band observed in the absorption spectrum of this class of manganese complexes.[1] The highest excited state contributing to the UV broad band corresponds mainly to the $\sigma_{Mn-R} \rightarrow \pi^*_{DAB}$ excitation. The purpose of this work being a qualitative estimation of the spin−orbit effects in the low-lying excited states on going from the manganese to the rhenium complex, we shall not try to improve the calculation of the transition energies. The spin−orbit splitting of the triplet states is negligible in this molecule going from 0 to a few tens of wavenumbers (Table 1).

The spin−orbit interactions between the low-lying excited states of $Mn(H)(CO)_3$(H-DAB) are reported in Table 2. The pure character of the excited states of interest, either MLCT or SBLCT, enables us to use a qualitative description of the first-order SO interaction based on the orientation of the orbitals involved in the electronic transition.[32] Indeed, the ^{1}SBLCT → ^{3}MLCT transition which is accompanied by the jump of one electron from the $3d_{xz}$ (xz oriented) to the σ_{Mn-H} orbital (z oriented) will generate orbital angular momentum along the Mn−H bond. This transition will be more efficient than the ^{1}SBLCT → ^{3}SBLCT transition for wich there is no such a spin-flip possibility (Scheme 1).

This is illustrated by the relatively high value of SOC in the former case (100 cm^{-1}) compared to the latter one (0 cm^{-1}). This large interaction of 100 cm^{-1}, calculated for the d^1A'−a^3A' (^{1}SBLCT−a^3MLCT) spin−orbit matrix element, should affect neither the absorption spectrum nor the photochemistry of the molecule regarding the large energy gap (12 940 cm^{-1}) between these two states and the absence of crossings on the related potential energy surfaces (Figure 1). A spin−orbit interaction of 75 cm^{-1} has been calculated between the c^1A' (MLCT) singlet state initially populated under visible irradiation and the c^3A' (SBLCT) state dissociative for the Mn−H bond homolysis.[12] These two states playing an important part both in the absorption spectrum and in the photochemical mechanism, an evaluation of this spin−orbit interaction has been performed as a function of the Mn−H bond distance (Figure 3) in order to investigate the SOC effect on the manganese−hydrogen bond homolysis.

The curves represented in Figure 3a show the evolution of the SOC between the b^1MLCT state, initially populated under visible irradiation,[11] and the ^{3}SBLCT state (upper curve Figure 3a) and between the b^1MLCT and the a^3MLCT state (lower curve Figure 3a) as a function of q_a = Mn−H. The shape of the b^1MLCT, a^3MLCT, and ^{3}SBLCT potential energy curves along the Mn−H bond elongation is represented in Figure 3b. These potential energy curves have been obtained through a cut along the Mn−H bond elongation into the whole set of two-dimensional PES [33] calculated as a function of the two coordinates q_a = Mn−H and q_b = Mn−Co_{axial} (Figure 1).

The evolution of the SOC follows the change of character of the two triplet states which is due to the avoided crossing

TABLE 2: Calculated Spin−Orbit Interaction (in cm^{-1}) in $Mn(H)(CO)_3(H\text{-}DAB)$ at the CASSCF/SOC-CI Level ($Z_{eff} = 15.0$)

	a^3A' ($3d_{xz} \rightarrow \pi^*$dab) a^3MLCT	b^3A' ($3d_{x^2-y^2} \rightarrow \pi^*$dab) b^3MLCT	c^3A' ($\sigma_{Mn-H} \rightarrow \pi^*$dab) ^{3}SBLCT
a^1A' (ground state)	20	60	70
b^1A' ($3d_{x^2-y^2} \rightarrow \pi^*$dab) a^1MLCT	80	20	20
c^1A' ($3d_{xz} \rightarrow \pi^*$dab) b^1MLCT	45	60	75
d^1A' ($\sigma_{Mn-H} \rightarrow \pi^*$dab) ^{1}SBLCT	100	8	0

SCHEME 1

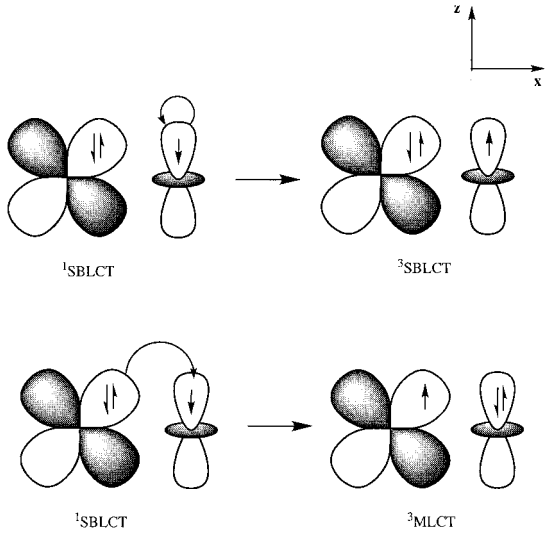

situated around 2.2 Å. This simplified representation of the complicated set of potential energy curves which describe the Mn−H bond homolysis in this molecule (Figure 1) does not take into account the other ^{1,3}MLCT states which should not modify significantly the following qualitative interpretation.

In the Franck−Condon region the two triplet states are nearly pure and well separated. Both interact through SOC with the ^{1}MLCT state initially populated under visible irradiation, with estimated values of 45 cm^{-1} for the ^{3}MLCT and 75 cm^{-1} for the ^{3}SBLCT. When the metal−hydrogen bond is elongated, the mixing between the two triplet states increases until the avoided crossing point. Accordingly, the ^{1}MLCT/^{3}SBLCT SOC decreases (since the ^{3}SBLCT state gains some MLCT character) whereas the ^{1}MLCT/^{3}MLCT SOC increases (since the ^{3}MLCT gains some SBLCT character) until dissociation where the two triplet states are again pure and well separated but reversed. The ^{1}MLCT → ^{3}SBLCT transition which populates the dissociative state with respect to the Mn−H bond breaking becomes more efficient as the metal−hydrogen bond is elongated. Consequently the metal−hydrogen bond homolysis should be assisted by spin−orbit coupling effects. In order to verify this hypothesis, preliminary one-dimensional simulations (along q_a = Mn−H) of the photodissociation dynamics of $Mn(H)(CO)_3$-(H-DAB) through wave packet propagations on the spin−orbit coupled potentials corresponding to the excited states reported in Table 1 have been performed in the diabatic representation.[10] The initial wave packet is prepared on the b^1MLCT state on the basis of the vibrational ground state of the electronic ground state with no amplitude on the low-lying triplet states at time t = 0. The potential coupling (spin−orbit) between the singlet and triplet potentials has been kept constant to 80 cm^{-1}.

According to these simulations, the probability of indirect dissociation via b^1MLCT → ^{3}SBLCT intersystem crossing is extremely low (close to 0.0) in the manganese complex in the picosecond time scale (Figure 4). This mechanism is not competitive with the direct dissociative deactivation channels (CO loss) which occurs within 200 fs.[34] At this level of the simulation other dissociative pathways have to be explored on the basis of multidimensional PES and relaxation effects have to be taken into account in the simulation (vibrational relaxation, solvent). This is beyond the scope of the present study.

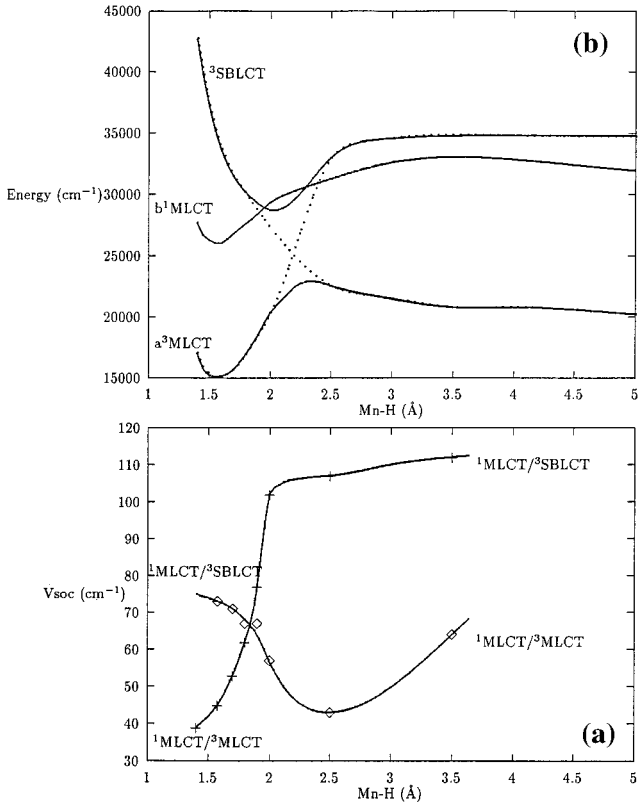

Figure 3. (a, bottom) Evolution of the spin−orbit coupling (SOC) between the b^1MLCT state and the ^{3}SBLCT state (upper curve on the left) and the a^3MLCT (lower curve on the left) as a function of q_a = [Mn−H]; (b, top) Shape of the b^1MLCT, a^3MLCT, and ^{3}SBLCT PEC along the Mn−H homolysis.

Spin−Orbit Effects in $Re(H)(CO)_3(H\text{-}DAB)$. The CASSCF/SOC-CI and CASSCF/MR-CCI excitation energies to the low-lying singlet and triplet states of $Re(H)(CO)_3(DAB)$ are reported in Table 3.

In order to estimate the correlation effects, the transition energies calculated at the CASSCF level using relativistic ECP nodeless pseudo-orbitals,[35] incompatible with the spin−orbit operator of eq 1 but used in the CASSCF/MR-CCI calculations, are also reported in Table 3. The corrections to the excitation energies do not exceed 9% on going from the CASSCF to the CASSCF/MR-CCI calculations. The SOC-CI values compare rather well with the CASSCF values, indicating a very small influence of the type of ECP (Stuttgart nodeless pseudo-orbitals or AIMP nodes showing pseudo-orbitals) used in the calcula-

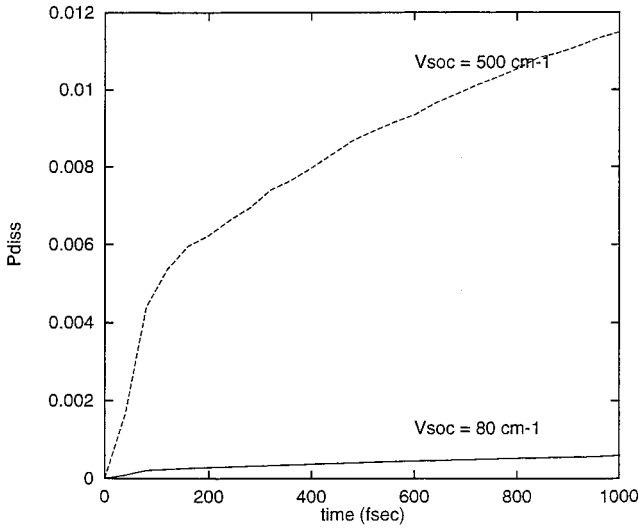

Figure 4. Probability of indirect dissociation of $Mn(H)(CO)_3$(H-DAB) via the b^1MLCT → ^{3}SBLCT intersystem crossing as a function of time.

TABLE 3: CASSCF/SOC-CI and CASSCF/MR-CCI Excitation Energies (in cm^{-1}) to the Low-Lying ^{1,3}A′ Excited States of Re(H)(CO)$_3$(H-DAB) and Spin−Orbit (SO) Splitting (in cm^{-1})

transition	CASSCF/-SOC-CI	SO splitting	CASSCF[a]	CASSCF/-MR-CCI[a]
$a^1A' \rightarrow a^3A'$				
MLCT	11 240	1160−1230	11 100	13 710
$a^1A' \rightarrow b^3A'$				
MLCT/SBLCT	12 160	280−310	13 750	12 600
$a^1A' \rightarrow b^1A'$				
MLCT	11 350	0	14 700	15 250
$a^1A' \rightarrow c^1A'$				
MLCT/SBLCT	21 370	0	21 700	21 720
$a^1A' \rightarrow c^3A'$				
SBLCT/MLCT	24 940	80−100	25 390	27 650
$a^1A' \rightarrow d^1A'$				
SBLCT/MLCT	28 640	0	29 840	31 340

[a] Reference 9.

tions. The only exception is the b^1A' excited state which is calculated at 11 350 cm^{-1} with the AIMP and at 14 700 cm^{-1} with the Stuttgart ECP (CAS level). The MR-CCI value of 15 250 cm^{-1} indicates that this could be an artifact of the ECP calculation using the AIMP. Indeed, it has been shown recently that some errors in the excitation energies can be traced to the matrix representation of the exchange operator.[36] The difference between the transition energies calculated at the CASSCF level and at the MR-CCI level is less important than in the manganese complex (Table 1), pointing to smaller correlation effects in third-row transition metal complexes (especially those related to the $d\pi-p\pi$ back-bonding in the metal−carbonyl bonds). The mixed character of the so-called MLCT and SBLCT excited states is well reproduced in the SOC-CI treatment. This point is very important regarding the influence of the molecular states composition on the spin−orbit matrix elements.

The spin−orbit splitting of the low-lying a^3A' state wich is purely MLCT is greater than 1000 cm^{-1}, much more significant than in the manganese complex. Values of a few hundred of wavenumbers have been calculated for the two other $^3A'$ excited states of mixed character MLCT/SBLCT. The SO splitting increases with the MLCT character of the triplet states due to the important metal contribution. The values reported in Table 3 agree with a magnitude of the zero-field splitting of the order of 100−1000 cm^{-1} (depending on the central metal atom) predicted for the MLCT states in transition metal complexes.[37]

The spin−orbit interactions between the low-lying singlet and triplet excited states of $Re(H)(CO)_3$(H-DAB) are reported in Table 4. A qualitative discussion based on the molecular orbitals involved in the electronic transition is untimely, regarding the mixed character of the electronic states in $Re(H)(CO)_3$(H-DAB). However, one may notice relatively low values of SO interaction for the singlet/triplet pairs for which there is no possibility of orbital jump generating orbital angular momentum along the Re−H bond. This is illustrated by the values of 100, 127, and 158 cm^{-1} for the $b^1A'-a^3A'$, $c^1A'-b^3A'$, and $d^1A'-c^3A'$, respectively. The largest value of 560 cm^{-1} has been calculated for the $b^1A'-a^3A'$ interaction between the pure ^{1}MLCT state and the mixed ^{3}(MLCT/SBLCT) state. The SOC between the ^{1}(MLCT/SBLCT) state contributing mainly to the visible absorption band and the ^{3}(SBLCT/MLCT) dissociative state with respect to the Re−H bond homosysis is estimated at 314 cm^{-1} in the Franck−Condon region. Values of 261 and 117 cm^{-1} have been proposed for the spin−orbit interaction between CT and ligand centered (LC) excited states in the related complexes $[Re(bpy)(CO)_4](PF_6)$ and $[Re(CO)_4(ppy)]$ (ppy = 2-phenylpyridine), respectively.[38]

The evolution of the SO interaction was followed as a function of the Re−H bond elongation. According to these calculations, the SO interaction never exceeds 580 cm^{-1} and the magnitude of the matrix elements follows the excited states composition evolution as illustrated in the manganese complex (Figure 3).

As a preliminary study of the SO effect on the indirect metal−hydrogen bond homolysis via intersystem crossing, the simulation reported for the manganese complex has been reproduced with a value of spin−orbit coupling of 500 cm^{-1}, close to the values obtained for the rhenium compound. According to this simulation, this process is very inefficient in the picosecond time scale, the probability of dissociation via the triplet state being less than 2% (Figure 4). It is worth noting that the shape of the potentials will differ on going from the manganese to the rhenium complex and will largely influence the dynamics. The calculation of the PES corresponding to the electronic ground state and low-lying excited states of $Re(H)(CO)_3$(H-DAB) is in progress. Nevertheless, this preliminary simulation on idealized potentials based on the PES calculated for the manganese complex agrees with a very low quantum yield ($\phi = 10^{-2}$) for the metal−methyl bond homolysis in the methyl analogue $Re(CH_3)(CO)_3$(H-DAB).[7]

4. Conclusion

The spin−orbit coupling effects on the metal−hydrogen bond homolysis of $M(H)(CO)_3$(H-DAB) (M = Mn, Re) have been investigated through SOC-CI, using a one-electron spin−orbit operator at the metal center and based on CASSCF wave functions. The present study has focused on the spin−orbit interaction between the low-lying singlet and triplet MLCT and SBLCT states corresponding to $nd \rightarrow \pi^*_{DAB}$ and $\sigma_{M-R} \rightarrow \pi^*_{DAB}$ excitations, respectively, which play a key role in the photochemistry of this class of molecules.

The SO splitting of the molecular triplet states is negligible in the managanese complex (a few tens of cm^{-1}) whereas it can reach a value of 1000 cm^{-1} for the low-lying ^{3}MLCT state in the rhenium analogue (heavy atom effect). It is important to realize that the SO splitting of the molecular states in a complex is rather low comparatively to the splitting observed or calculated in third-row transition metal atoms. This is the consequence of the electronic delocalization over the surrounding ligands. Moreover, the SO splitting decreases significantly

TABLE 4: Calculated Spin−Orbit Interaction (in cm^{-1}) in $Re(H)(CO)_3(H\text{-}DAB)$ at the CASSCF/SOC-CI Level ($Z_{eff} = 60.0$)

	a^3A' ($5d_{x^2-y^2} \rightarrow \pi^*_{dab}$) MLCT	b^3A' ($5d_{xz}/\sigma_{Re-H} \rightarrow \pi^*_{dab}$) MLCT/SBLCT	c^3A' ($\sigma_{Re-H}/5d_{xz} \rightarrow \pi^*_{dab}$) SBLCTMLCT
a^1A' (ground state)	370	188	369
b^1A' ($5d_{x^2-y^2} \rightarrow \pi^*_{dab}$) a^1MLCT	158	560	233
c^1A' ($5d_{xz}/\sigma_{Re-H} \rightarrow \pi^*_{dab}$) MLCT/SBLCT	532	127	314
d^1A' ($\sigma_{Re-H}/5d_{xz} \rightarrow \pi^*_{dab}$) SBLCT/MLCT	151	393	100

(10%) in mixed ^{3}MLCT/SBLCT states which lose metal character with respect to pure MLCT states.

The pure character of the excited states of interest in $Mn(H)(CO)_3(H\text{-}DAB)$, either MLCT or SBLCT, makes valid a qualitative analysis of the singlet−triplet SO interaction, based on the orientation of the orbitals involved in the electronic transition participating to the singlet−triplet intersystem crossing. Thus, the ^{1}SBLCT → ^{3}MLCT transition appears to be more efficient than the ^{1}SBLCT → ^{3}SBLCT transition for which there is no spin-flip possibility during the electronic jump associated to the intersystem crossing process. This hypothesis is corroborated by the calculated SO interactions between the ^{1}SBLCT and the ^{3}MLCT on one hand (100 cm^{-1}) and between the ^{1}SBLCT and the ^{3}SBLCT on the other hand (0 cm^{-1}). An intermediate value of 75 cm^{-1} has been obtained for the spin−orbit coupling between the ^{1}MLCT state, initially populated under irradiation in the visible and the ^{3}SBLCT state, dissociative for the manganese−hydrogen bond homolysis. An increase in the efficiency of the ^{1}MLCT → ^{3}SBLCT intersystem crossing process as a function of the metal−hydrogen bond elongation has been proposed. Preliminary wave packet propagations on the SO coupled potentials point to a slow (beyond the picosecond time scale) intersystem crossing process in the manganese complex, not competitive with the direct dissociative deactivation channel (CO loss) which occurs within a few hundred of femtoseconds.[9]

In contrast to the manganese complex, the mixed character (MLCT/SBLCT) of the low-lying excited states in $Re(H)(CO)_3(H\text{-}DAB)$ excludes a qualitative analysis based on molecular orbitals involved in the intersystem crossing process. However, one may notice relatively low values of SO interaction for the singlet/triplet pairs for which there is no possibility of orbital jump generating orbital angular momentum along the Re−H bond. Surprisingly, the SO interactions in the rhenium complex never exceed 580 cm^{-1} and a value of 360 cm^{-1} has been obtained for the interaction between the ^{1}MLCT state, initially populated and the ^{3}(SBLCT/MLCT) state, dissociative with respect to the Re−H bond homolysis, in the Franck−Condon region. As in the manganese complex and in the limit of the preliminary simulation, the intersystem crossing process, which populates this state leading to the formation of the homolysis primary products, is very inefficient in the picosecond time scale. At this stage of the theoretical study one may predict a low effeiciency of the metal−hydrogen bond homolysis in both model complexes $Mn(H)(CO)_3(H\text{-}DAB)$ and $Re(H)(CO)_3(H\text{-}DAB)$ in agreement with the low quantum yields proposed for the methyl analogues, $\phi = 0$ and $\phi = 10-2$, respectively.

Further work will include an improovement of the spin−orbit operator and relaxation effects (structural deformation, solvent effects on excited states dynamics) competitive with intersystem crossing processes which seem to occur within picosecond to nanosecond time scales in the complexes investigated in the present study.

Acknowledgment. The authors are grateful to Dr. M. R. Hachey and to W. Cardoen for helpful discussions. Generous financial support from the European Community and from the CNRS for the COST D4/00194/ project entitled "Design and preparation of new molecular systems with unconventional electrical, optical and magnetic properties" is gratefully acknowledged. B.M. acknowledges the INTAS project "Theory and application of spin-catalysis" for a visiting grant. The calculations were carried out on the C98 computer of the IDRIS (Orsay, France) through a grant of computer time from the Conseil Scientifique, on the workstations of the division of Quantum Chemistry (Leuven) and the Laboratoire de Chimie Quantique (Strasbourg).

References and Notes

(1) Stufkens, D. J. *Comments Inorg. Chem.* **1992**, *13*, 359.
(2) Stufkens, D. J. *Coord. Chem. Rev.* **1990**, *104*, 39.
(3) Rossenaar, B. D.; van der Graaf, T.; van Eldick, R.; Langford, C. H.; Stufkens, D. J.; Vlček, A., Jr. *Inorg. Chem.* **1994**, *33*, 2865.
(4) Rossenaar, B. D.; Kleverlaan, C. J.; Stufkens, D. J.; Oskam, A. *J. Chem. Soc., Chem. Commun.* **1994**, 63.
(5) van Outerstep, T. W. M.; Stufkens, D. J.; Vlček, A., Jr. *Inorg. Chem.* **1995**, *34*, 5183.
(6) Rossenaar, B. D.; George, M. W.; Johnson, F. P. A.; Stufkens, D. J.; Turner, J. J.; Vlček, A., Jr. *J. Am. Chem. Soc.* **1995**, *117*, 11 582.
(7) . Rossenaar, B. D.; Kleverlaan, C. J.; van de Ven, M. C. E.; Stufkens, D. J.; Vlček, A., Jr. *Chem. Eur. J.* **1996**, *2*, 228.
(8) Rossenaar, B. D.; Stufkens, D. J.; Oskam, A.; Fraanje, J.; Goubitz, K. *Inorg. Chim. Acta* **1996**, *247*, 215. Rossenaar, B. D.; Lindsay, E.; Stufkens, D. J.; Vlček, A., Jr. *Inorg. Chim.* Acta **1996**, *250*, 5.
(9) Guillaumont, D.; Wilms, M. P.; Daniel, C.; Stufkens, D. J. *Inorg. Chem.* **1998**, *37*, 5816.
(10) Guillaumont, D.; Finger, K.; Hachey, M. R.; Daniel, C. *Coord. Chem. Rev.* **1998**, *171*, 439.
(11) Guillaumont, D.; Daniel, C. *Coord. Chem. Rev.* **1998**, *177*, 181.
(12) Finger, K.; Daniel, C. *J. Chem. Soc., Chem. Commun.* **1995**, 63. Finger, K.; Daniel, C. *J. Am. Chem. Soc.* **1995**, *117*, 12 322.
(13) Finger, K.; Daniel, C.; Saalfranck, P.; Schmidt, B. *J. Phys. Chem.* **1996**, *110*, 3368.
(14) Kleverlaan, C. J.; Stufkens, D. J. *Inorg. Chim. Acta*, in press. Kleverlaan, C. J.; Stufkens, D. J.; Clark, I. P.; George, M. W.; Martinoe, D. M.; van Willigen, H.; Vlček, A., Jr. *J. Am. Chem. Soc.* **1998**, *120*, 10871.
(15) Kleverlaan, C. J. Ph.D. Thesis, University of Amsterdam, The Netherlands, 1998. Rossenaar, B. D. Ph.D. Thesis, University of Amsterdam, The Netherlands, 1995.
(16) Schmidt, G. S.; Paulus, H.; van Eldick, R.; Elias, H. *Inorg. Chem.* **1988**, *27*, 3211.
(17) Mc Neill, E. A.; Schöler, F. R. *J. Am. Chem. Soc.* **1977**, *99*, 66243.
(18) Rossenaar, B. D.; Kleverlaan, C. J.; van de Ven, M. C. E.; Stufkens, D. J.; Oskam, A.; Fraanje, J.; Goubitz, K. *J. Organomet. Chem.* **1995**, *493*, 153.
(19) Guillaumont, D.; Daniel, C. *Chem. Phys. Lett.* **1996**, *257*, 1.
(20) This basis set is made from the (14,9,5) basis set of Wachters,[21] by adding an additional s function (exponent 0.3218), two diffuse p functions, and one diffuse d function. All the exponents were chosen according to the even-tempered criterion of Raffenetti.[22]
(21) Wachters, A. J. H. *J. Chem. Phys.* **1970**, *52*, 1033.
(22) Raffenetti, R. C.; Bardo, R. D.; Ruedenberg, K. In *Energy Structure and Reactivity*; Smith, D. W., McRae, W. B., Eds.; Wiley: New York, 1973; p 164.
(23) Huzinaga, S. *Approximate Atomic Functions;* technical report; University of Alberta, Canada, 1971.
(24) Huzinaga, S. *J. Chem. Phys.* **1965**, *42*, 1293.

(25) Barandiaran, Z.; Seijo, L.; Huzinaga, S. *J. Chem. Phys.* **1990**, *93*, 5843.

(26) Pierloot, K.; Dumez, B.; Widmark, P.-O.; Roos, B. O. *Theor. Chim. Acta* **1995**, *90*, 87.

(27) Siegbahn, P. E. M.; Almlöf, J.; Heiberg, A.; Roos, B. O. *J. Chem. Phys.* **1981**, *74*, 2384.

(28) Ribbing, C.; Daniel, C. *J. Chem. Phys.* **1994**, *100* (9), 6591.

(29) Moore, C. E. *Atomic Energy Levels;* Natl. Bur. Stand. Circ. No. 467, 1952.

(30) *Molcas 3.0:* Andersson, K.; Blomberg, M. R. A.; Fülscher, M. P.; Karström, G.; Kellö, V.; Lindh, R.; Malmqvist, P.-Å.; Noga, J.; Olsen, J.; Roos, B. O.; Sadlej, A. J.; Siegbahn, P. E. M.; Urban, M.; Widmark, P.-O. University of Lund, Sweden.

(31) Ernenwein, R.; Rohmer, M. M.; Bénard, M. *Comput. Phys. Commun.* **1990**, *58*, 305. Wiest, R.; Demuynck, J.; Bénard, M.; Rohmer, M. M.; Ernenwein, R. *Comput. Phys. Commun.* **1991**, *62*, 107.

(32) Turro, N. J. In *Modern Molecular Photochemistry*; The Benjamin/Cummings Publishing Co. Inc.: New York, 1978.

(33) Guillaumont, D.; Daniel, C., submitted.

(34) Daniel, C.; Heitz, M. C.; Lehr, L.; Schröder, T.; Warmuth, B. *Int. J. Quantum Chem.* **1994**, *52*, 71.

(35) Andrae, D.; Haeussermann, U.; Dolg, M.; Stoll, H.; Preuss, H. *Theor. Chim. Acta* **1990**, *77*, 123. Bergner, A.; Dolg, M.; Kuechle, W.; Stoll, H.; Preuss, H. *Mol. Phys.* **1993**, *80*, 1431.

(36) Rakowitz, F.; Marian, C. M.; Seijo, L.; Wahlgren, U. *J. Chem. Phys.*, in press. Marian, C. M. private communication.

(37) Azumi, T.; Miki, H. *Topics in Current Chemistry Vol. 171*; Yersin, H., Ed.; Spring Verlag: Berlin, 1997; pp 1−40.

(38) Strouse, G. F.; Güdel, H. U. *Inorg. Chem.* **1995**, *34*, 5578. Vanhelmont, F. W. M.; Strouse, G. F.; Güdel, H. U. *J. Phys. Chem. A* **1997**, *101*, 2946.